Pediatric Nephrology
https://doi.org/10.1007/s00467-022-05634-x

ORIGINAL ARTICLE

Focal segmental glomerulosclerosis and proteinuria associated with *Myo1E* mutations: novel variants and histological phenotype analysis

Mira Krendel[1] · Sabine Leh[2,3] · Michael E. Garone[1] · Alcia Edwards-Richards[4] · Jen-Jar Lin[4] · Damien Brackman[5] · Per Knappskog[6,7] · Alexei Mikhailov[8]

Received: 28 November 2021 / Revised: 8 May 2022 / Accepted: 11 May 2022

Abstract

Background Pathogenic mutations in the non-muscle single-headed myosin, myosin 1E (Myo1e), are a rare cause of pediatric focal segmental glomerulosclerosis (FSGS). These mutations are biallelic, to date only reported as homozygous variants in consanguineous families. Myo1e regulates the actin cytoskeleton dynamics and cell adhesion, which are especially important for podocyte functions.

Methods DNA and RNA sequencing were used to identify novel *MYO1E* variants associated with FSGS. We studied the effects of these variants on the localization of Myo1e in kidney sections. We then analyzed the clinical and histological observations of all known pathogenic *MYO1E* variants.

Results We identified a patient compound heterozygote for two novel variants in *MYO1E* and a patient homozygous for a deletion of exon 19. Computer modeling predicted these variants to be disruptive. In both patients, Myo1e was mislocalized. As a rule, pathogenic *MYO1E* variants map to the Myo1e motor and neck domain and are most often associated with steroid-resistant nephrotic syndrome in children 1–11 years of age, leading to kidney failure in 4–10 years in a subset of patients. The ultrastructural features are the podocyte damage and striking diffuse and global Alport-like glomerular basement membrane (GBM) abnormalities.

Conclusions We hypothesize that *MYO1E* mutations lead to disruption of the function of podocyte contractile actin cables resulting in abnormalities of the podocytes and the GBM and dysfunction of the glomerular filtration barrier. The characteristic clinicopathological data can help to tentatively differentiate this condition from other genetic podocytopathies and Alport syndrome until genetic testing is done.

Keywords Myo1e · *MYO1E* · Non-muscle myosin · Focal segmental glomerulosclerosis (FSGS) · Actin cables · Glomerular basement membrane multilayering · Alport-like

✉ Alexei Mikhailov
avmikhai@wakehealth.edu

[1] Department of Cell and Developmental Biology, SUNY Upstate Medical University, Syracuse, NY, USA

[2] Department of Pathology, Haukeland University Hospital, Bergen, Norway

[3] Department of Clinical Medicine, University of Bergen, Bergen, Norway

[4] Department of Pediatrics, Wake Forest Baptist Medical Center, Winston-Salem, NC, USA

[5] Department of Pediatrics, Haukeland University Hospital, Bergen, Norway

[6] Department of Clinical Science, University of Bergen, Bergen, Norway

[7] Department of Medical Genetics, Haukeland University Hospital, Bergen, Norway

[8] Department of Pathology, Atrium Health Wake Forest Baptist Medical Center, Winston-Salem, NC, USA

Published online: 20 June 2022

Introduction

Focal segmental glomerulosclerosis (FSGS) is a histomorphological pattern of glomerular injury associated with proteinuria. Primarily a podocytopathy, FSGS is currently subdivided into three etiological variants: primary, secondary, and genetic. Genetic FSGS presents clinically as steroid-resistant proteinuria in children (typically autosomal recessive) or adults (mostly autosomal dominant) and is caused by mutations in proteins essential for podocyte development, structure, and function. Although genetic FSGS appears clinicopathologically uniform, limited available observations of some rare etiologies, such as mutations in a structural protein Myo1e, reveal unexpected features that may facilitate the diagnosis and further our understanding of FSGS.

Myo1e is a non-muscle class I (one-headed) myosin which plays a role in the organization of the actin cytoskeleton, vesicle trafficking, and in the regulation of tension between the plasma membrane and the cytoskeleton [1]. Myo1e consists of actin- and ATP-binding motor/head domain, a calmodulin-binding neck domain that acts as a lever coupling the conformational changes in the motor domain to the physical movement, and a C-terminal tail domain (Fig. 1). The tail homology (TH1) domain is responsible for the interaction with cell membranes. Of the eight myosin 1 isoforms identified in humans, the widely expressed Myo1e is important specifically for normal kidney function. In the glomerulus, Myo1e colocalizes with synaptopodin-labeled actin filament bundles at podocyte foot processes [2] and with cell adhesion protein ZO-1 at the slit diaphragm [3]. Myo1e knockout results in proteinuria, podocyte foot process effacement, and disorganization of the glomerular basement membrane (GBM) resulting specifically from podocyte Myo1e inactivation [4]. Since the first Myo1e mutations were reported in children with FSGS in 2011 [5], only 6 homozygous variants of Myo1e in 9 pediatric patients with steroid-resistant proteinuria and FSGS have been identified.

Here, we report two patients with novel *MYO1E* variants, and in conjunction with the literature data, we summarize the clinicopathological features of the disease.

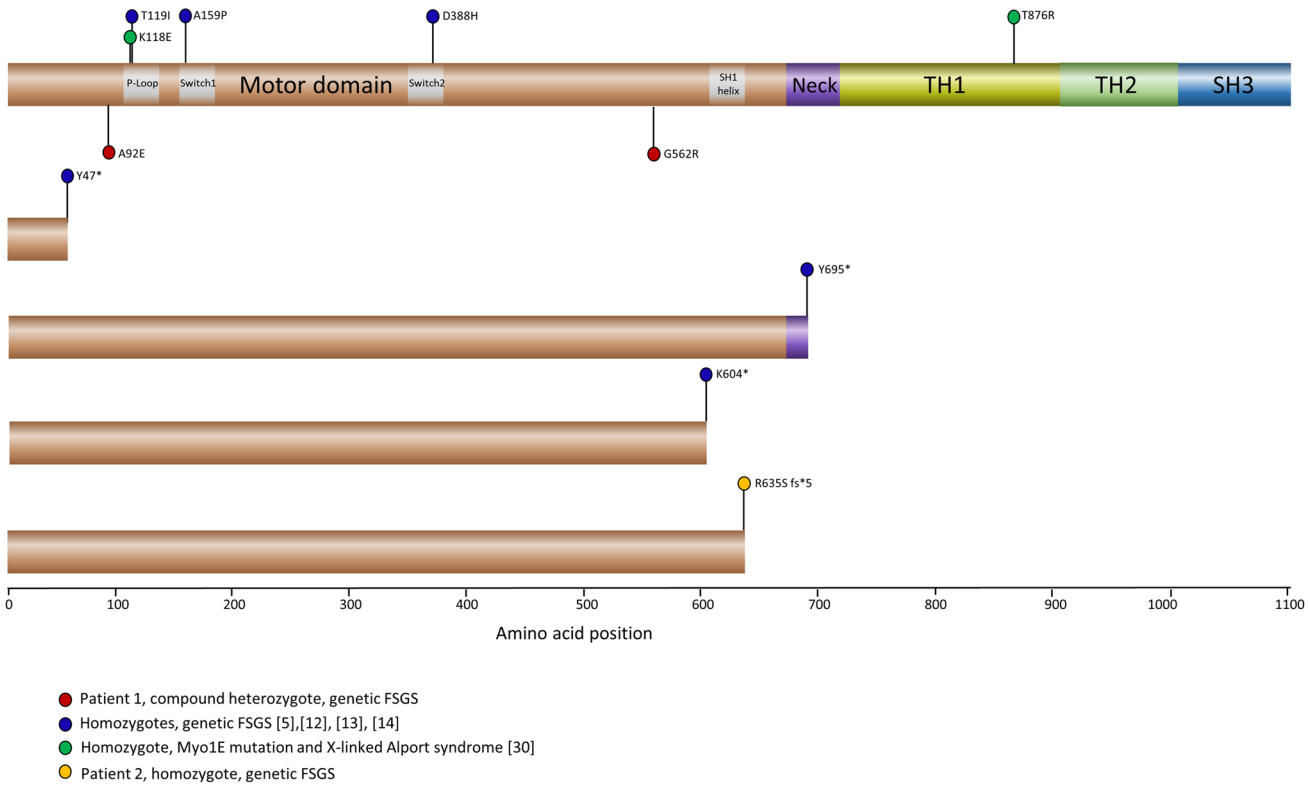

Fig. 1 The non-muscle Class I myosin Myo1e and the schematic of known FSGS-associated variants indicating their position across the functional domains of Myo1e, with each variant represented by a circle colored according to the table at the bottom. TH1 and 2, the tail homology 1 and 2 domains; SH3, the Src-homology 3 domain

Methods

Pathologic analysis

Kidney core biopsy tissue was processed and evaluated with standard clinical methods for light, immunofluorescence (patient 1), immunohistochemistry (patient 2), and electron microscopy. Patient 2 was biopsied twice. The first biopsy was at 10 years of age; the electron microscopy sample was reprocessed from formalin fixed paraffin-embedded tissue and showed numerous artifacts. The second biopsy was at the age of 12 years.

Fluorescence microscopy

The frozen 5-µm cryostat sections of a control kidney biopsy, kidney biopsies of patient 1, and a patient with minimal change disease (MCD) were co-stained with rabbit antibodies to human Myo1e tail (amino acids 721–1109) ([6], RRID AB_2909514) and mouse monoclonal antibodies to human synaptopodin (clone G1D4, GeneTex, Irvine, CA, RRID AB_11161967), visualized using the Alexa Fluor 568 conjugated anti-rabbit and Alexa Fluor 488 conjugated anti-mouse antibodies (Thermo Fisher Scientific, Waltham, MA). The Myo1e antibody was previously validated using Myo1e knockout mouse tissue samples [2]. All staining was done at a dilution of 1:100 for 30 min. The sections were examined using an Olympus FluoView 1200 laser confocal microscope (Atrium Health Wake Forest Baptist Medical Center (AHWFBMC) Cellular Imaging Shared Resource). Two blinded observers independently scored images of anti-Myo1E-stained glomeruli and reliably sorted the images from the control biopsy samples and the patient samples in two groups, confirming that differences in Myo1e localization were readily identifiable. The extent of colocalization of the Myo1e and synaptopodin signal was measured from the confocal images (2 images per sample) using the co-loc2 plugin in Fiji [7].

Heat-induced epitope retrieval was performed on the control patient and patient 2 deparaffinized sections in citrate buffer pH 6.0 in a pressure cooker. Immunostaining was performed as above, except an HPA023886 rabbit antibody against amino acids 966–1098 (MilliporeSigma, Burlington, MA, RRID AB_1854253) was used to visualize Myo1e. A positive immunofluorescence signal for both target proteins was obtained in the control specimen after a 40-min incubation. With patient 2 sections, incubation times from 20 min to 3 h were tested. Synaptopodin staining was best at 2 h with longer incubation times resulting in signal degradation.

Genetic analysis

The samples were collected following informed consent. Patient 1: The sequence analysis by next-generation sequencing and copy number testing of 17 genes (*ACTN4*, *ANLN*, *CD2AP*, *COL4A3*, *COL4A4*, *COL4A5*, *CRB2*, *HNF1A*, *INF2*, *LMX1B*, *MYO1E*, *NPHS1*, *NPHS2*, *PAX2*, *PKDZ*, *PKHD1*, *TRPC6*) was performed by Invitae, Inc. (San Francisco, CA). Patient 2: The SNP-chip analysis was performed using the 250 K Affymetrix SNP-array on DNA. Candidate genes were sequenced by Sanger sequencing using DNA and/or RNA as a template. DNA and RNA were purified from blood using standard methods.

Results

A total of 136 patients with steroid-resistant proteinuria and suspicion for genetic FSGS underwent genetic testing at the Haukeland University Hospital, Bergen, Norway, since the University started offering testing for Myo1e. Fifty-four such patients were tested at the Atrium Health North Carolina institutions. Two pediatric patients with Myo1e mutations were identified.

Family 1

The proband (patient 1) 1 is an 11-year-old boy with an incidental finding of proteinuria (Table 1). Other laboratory indicators of kidney function were normal. A kidney biopsy was performed 1 month later and demonstrated 3% global glomerulosclerosis and 10% segmental tuft sclerosis. The sclerosing segments were located at the urinary pole (Fig. 2a) and in other areas of the capillary tuft. Some of the non-sclerosed glomeruli were hypertrophic and hyperplastic, and some demonstrated segmental mild mesangial expansion and mild hypercellularity. Scattered foam cells were noted in the tubulointerstitial compartment (Fig. 2a), and small foci of interstitial fibrosis and tubular atrophy were seen. 3 + granular staining of IgA along a few glomerular peripheral capillary walls and in some mesangial zones, accompanied by minor (1 +) IgM and mild-to-moderate (2 +) lambda light chain staining, were present. A similar staining pattern has been reported in Myo1e-related FSGS [5] and is thought to have no pathogenetic significance. Antibodies to the Collagen type IV α1, α3, and α5 subunits displayed a normal staining pattern.

The ultrastructural examination of four glomeruli showed alternating areas of GBM thinning (Fig. 2b; measured GBM thickness was significantly less than that reported for children of 11 years of age (297 + / − 6 nm [8]) and irregular thickening with marked structural rearrangements such as splitting and basket-weaving of the lamina densa (Fig. 2e),

Table 1 Summary of clinical data from case 1 and 2 and published patients with Myo1e-associated FSGS

Source	Mutation	Age[1]	Age at the index biopsy	Age at kidney failure	Proteinuria[1]	Hematuria[1]	Serum creatinine, mg/dL[1]	Mesangial changes	Electron microscopy	Treatment	Treatment-associated change in proteinuria
Patient 1	A92E, G562R	11y	11y	n/a	1.1 g/m^2/day	None	0.6	Expansion	Yes	Steroids, ACE inhibitors	Reduction
Patient 2	R635Sfs*5	10y	10y	17y	3.4 g/24 h	Micro	0.6	Expansion	Yes	Steroids, ciclosporin	None
[5]	A159P	9y	9y	13y	3 g/24 h	Micro	0.6	Hyperplasia	No	Steroids, ciclosporin, ACE inhibitors	None
[5]	A159P	4y	4y	n/a	1.56 g/24 h	None	0.4	Hyperplasia	No	Ciclosporin, ACE inhibitors	Reduction on ciclosporin
[5]	A159P	2y	2y	n/a	3.4 g/24 h	None	0.4	Hyperplasia	No	Steroids, ciclosporin, ACE inhibitors	Reduction on ciclosporin
[5]	Y695*	1y	4y	n/a	"++++"	Yes	0.3	None	Yes	Steroids, ciclosporin, ACE inhibitors	Reduction on ciclosporin
[12], 3 patients	A159P	3–10 y.o	-	-	Nephrotic	-	-	-	No	-	-
[13]	Y47*	4 m	4 m	10y	Nephrotic	-	-	-	-	-	-
[13]	Y47*	3y	3y	4y to CKD1	Nephrotic	-	-	-	MCD	-	-
[13]	T119I	8y	8y	12y	Nephrotic	-	-	-	-	-	-
[14]	K604*	1 y 8 m	-	-	Nephrotic	-	-	-	-	Steroids, ciclosporin	None
[14]	D388H	7y	10y	-	Nephrotic	-	-	-	-	Steroids, cyclophosphamide, mycophenolate	None

n/a, kidney failure did not occur within the observation period (1–13 y); -, data not available

[1]At initial presentation

y, year; *m*, month

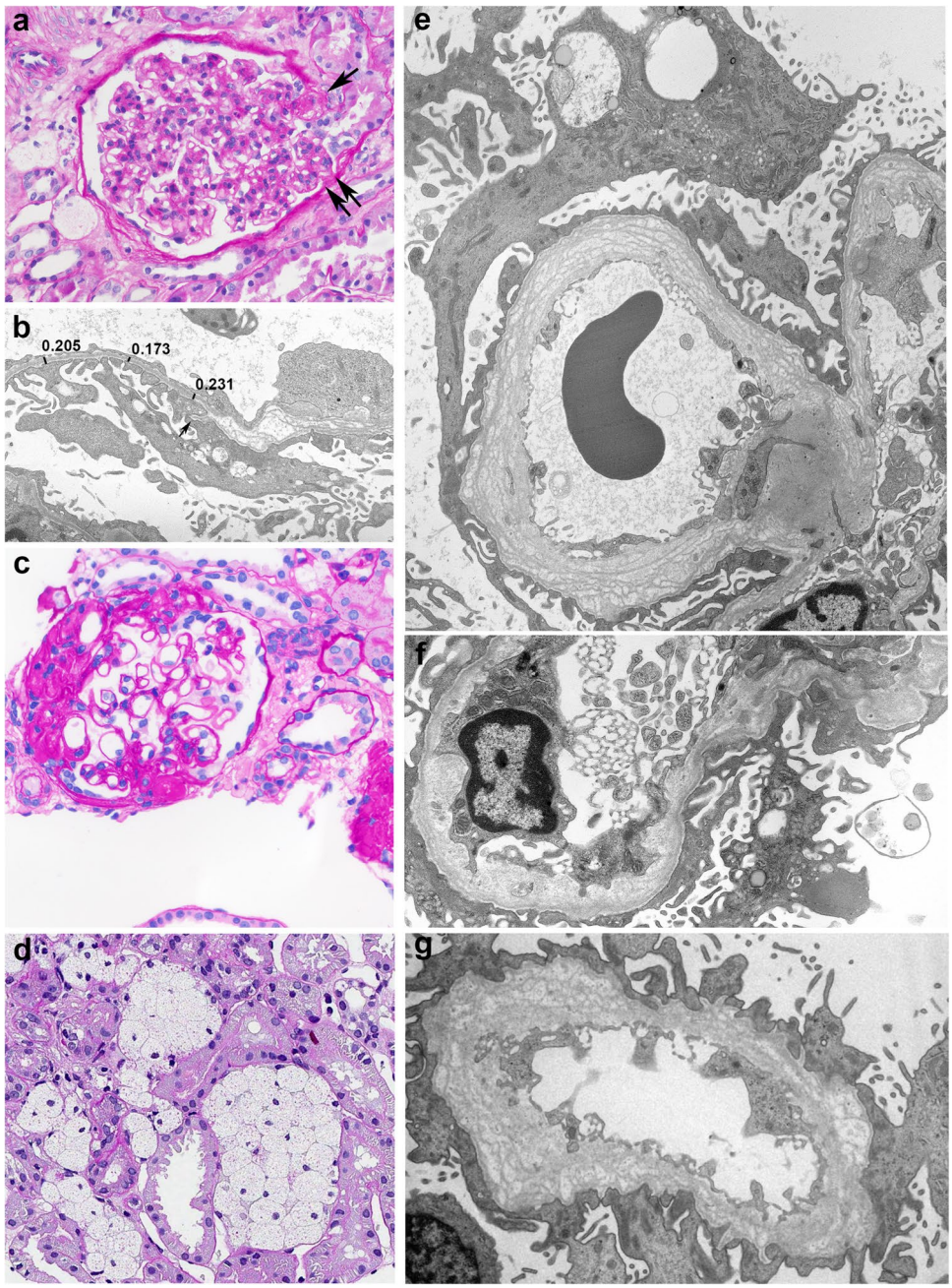

Fig. 2 Kidney biopsy, light (**a**, **c,** **d**), and transmission electron (**b**, **e**–**g**) micrographs. Patient 1 (**a**, **b**, **e**, **f**); patient 2 (**c**, **d**, **g**). **a** A sclerosed capillary segment attached to the Bowman's capsule (single arrow), and a cross-bridge between a tuft segment and the Bowman's capsule (double arrow). The glomerulus demonstrates a mild increase in mesangial matrix and segmental mesangial hypercellularity. Note interstitial foam cells to the left of the glomerulus. **b** GBMs are irregular, with thicker laminated and thinner portions. GBM width in thinner portions (black lines) indicated in μm. A GBM microspike (arrow). **c** Segmental sclerosis with several capillary segments solidified and attached to the Bowman's capsule. **d** Clusters of foam cells in the interstitium. **e** Alport-like ultrastructural lesion characterized by marked irregular thickening of the glomerular basement membrane with splitting and fragmenting of the lamina densa into multiple strands forming a basket-weave pattern, focally very marked and resembling "bubble wrap." The mesangial matrix is unaffected. The podocytes display large vacuoles, a condensed cytoplasm, microvillous transformation, and variable moderate-to-severe foot process effacement. **f** Irregular bulging of the lamina rara interna with electron-lucent areas containing vacuolar and cell process inclusions, GBM splitting, and a few electron dense deposits, alternating with foci of thinner GBM. **g** Alport-like ultrastructural lesion, similar to **e**. Marked irregular inner and especially outer contour of the GBM

bread crumb-like inclusions and rare electron dense deposits (Fig. 2f). Rare microspike-like subepithelial GBM projections were noted (Fig. 2b, arrow). Podocytes displayed moderate to severe foot process effacement and focal foot process detachment, microvillous transformation, pronounced cytoplasmic vacuolization, and shrinking. The extent of foot process effacement did not correlate with the severity of the underlying GBM changes. The podocyte slit diaphragms were preserved. A few capillary segments demonstrated moderate or marked mesangial matrix expansion and mild mesangial hypercellularity.

The patient's parents, unrelated, are both in their 50s and with no medical histories or complaints. Post-biopsy, the patient has received an angiotensin-converting enzyme inhibitor and high-dose steroids with improvement in proteinuria.

Family 2

The proband in family 2 (patient 2), 10 years old, was incidentally found to have proteinuria (Table 1). Serum albumin was 3.3 g/dL; there was a microhematuria of 5–15 red blood cells/high-power field. Other laboratory indicators of kidney function, audiometry, and eye examination were normal. There was 13% global and 19% segmental glomerulosclerosis. Mild mesangial expansion and hypercellularity were found in one non-sclerosed glomerulus. The interstitium contained numerous foam cells; tubular atrophy was minimal. The immunohistochemical study did not reveal immunoglobulin or complement deposition. An immunofluorescence study of a skin biopsy showed normal distribution of collagen IV α5 and α6 isoforms. An ultrastructural examination revealed thickening and lamellation of the GBM.

Steroids, cyclophosphamide, and ciclosporin in succession did not reduce the urine protein level or prevent the rise in blood pressure.

A second kidney biopsy at 12 years of age demonstrated similar findings. FSGS (Fig. 2c) and chronic tubulointerstitial changes had not increased; the non-sclerosed glomeruli were unremarkable. Numerous foam cells were present in the interstitium (Fig. 2d).

Irregular marked GBM thickening with the splitting of the lamina densa into interwoven thin layers, "bread crumbs," and marked irregularity of the inner and outer contours with microspike-like subepithelial projections (Fig. 2g) were seen under electron microscopy. Podocyte foot processes were segmentally effaced. Kidney function remained normal until 17 years of age when the $eGFR_{cr}$ started falling gradually. At the age of 22, the patient received a kidney transplant.

The patient's parents are related (cousins, five generations removed); there is no family history of kidney disease.

Genetic analysis

Genetic testing revealed that patient 1 was heterozygous for two missense variants in the *MYO1E* gene, A92E, and G562R (Table 2, Fig. 1). Both affected amino acid residues are located in the Myo1e motor domain and are highly conserved (Fig. 3). Since the crystal structure of mammalian

Table 2 Genetic testing of patients 1 and 2

				In silico predictive programs				
	Nucleotide changes in the *MYO1E* gene	Amino acid	Family history	REVEL	SIFT	PolyPhen 2	Variant frequency in gnomAD	ACMG classification
Patient 1	c.275C > A, exon 4	p.A92E	Variants detected in trans, each of the unaffected parents carries one of the variant alleles	0.89	Affects protein function	Probably damaging	None	VUS[1]
	c.1684G > A, exon 16	p.G562R		0.87	Affects protein function	Probably damaging	1 instance, heterozygous, frequency of 0.000003980	VUS[1]
Patient 2	r.1905_2049del145, deleted exon 19	p.R635S fs*5 (homozygous)	No family history of kidney disease, parents not tested				None	Pathogenic[2]

[1]Supporting evidence: PM2_Supporting, variant not detected in population databases; PP3_Moderate, in silico predictions support a deleterious effect on the gene or gene product; PP4, patient's phenotype is highly specific for a disease with a single genetic etiology

[2]Supporting evidence: PVS1 null variant (exon deletion) in a gene where loss of function is a known mechanism of disease; PM2_supporting, variant not detected in population databases; PP4, patient's phenotype is highly specific for a disease with a single genetic etiology

VUS, variant of unknown significance

Myo1e has not been determined, we mapped locations of two residues affected by the mutations onto the crystal structure of a class I myosin from the slime mold *Dictyostelium discoideum*, MyoIE [9] using UCSF Chimera [10]. Both amino acid residues are non-polar amino acids located within alpha-helical regions (Fig. 3d), which are replaced with charged residues in the mutated versions of Myo1e. The A92E mutation in *MYO1E* is homologous to a previously reported mutation in *MYO5B*, A143E, associated with the microvillus inclusion disease (MVID) [11].

Testing of the parents of patient 1 revealed the A92E variant in the father and the G562R variant in the mother. This finding is consistent with the recessive inheritance of Myo1e-associated FSGS, as previously reported [5]. No abnormalities were detected in the 16 other genes tested (see "Methods").

In patient 2, a genome-wide SNP analysis revealed a 20.8-Mb region of homozygosity on chromosome 15 containing the *MYO1E* gene. PCR amplification of exon 19 of the *MYO1E* gene failed, and DNA sequencing identified a transcript lacking exon 19 (Table 2, Fig. 1). This transcript is predicted to be translated into a truncated nonfunctional protein lacking the Myo1e neck and tail. The parents of patient 2 were not tested.

No pathogenic variants in the *COL4A3-COL4A5* genes were detected in either of the patients.

Myo1e immunolocalization

In the control glomeruli, the Myo1e immunostaining colocalized with synaptopodin in a linear and punctate pattern, lining the GBM and corresponding to the podocyte foot processes and the podocyte plasma membrane (Fig. 4a). Myo1e was also present in the podocyte cytoplasm, displaying diffuse and less intense staining. Colocalization between Myo1e and synaptopodin was reduced in the glomeruli of patient 1, with less Myo1e signal seen along the GBM and more in the cytoplasm (Fig. 4b). Pearson's correlation coefficient for the Myo1e and synaptopodin channels in images from the control samples ranged from 0.57 to 0.64, while in images from patient 1 samples, it was lower at 0.37–0.41. As Myo1e could be passively displaced from the podocyte–GBM interface due to foot process effacement, we compared the result seen in the patient with the *MYO1E* mutation to that in a patient with MCD. In MCD, Myo1e and synaptopodin still colocalized in a linear pattern along the GBM (Fig. 4c) in the effaced foot processes.

In preliminary experiments, we expressed EGFP-tagged Myo1e A92E in MDCK cells. The mutant protein was absent from the MDCK plasma membrane and cell–cell junctions (data not shown).

In patient 2, a Myo1e antibody directed against amino acids 966–1098 (see "Methods") failed to produce a convincing signal by immunofluorescence.

Clinical summary of all known Myo1e-associated FSGS patients

Nine *MYO1E* mutations, including the 3 novel variants discussed above (3 missense homozygotes, 4 nonsense homozygotes, and 2 missense compound heterozygotes), have been discovered in 11 pediatric patients with FSGS (Fig. 1 and Table 1).

MYO1E variants segregating with FSGS in humans (p.A159P and Y695*) were first described in two families in 2011 [5, 12] (4 patients; it appears that 3 of them studied in both works are the same). Subsequently, two additional *MYO1E* variants (Y47* and T119I) were reported in 2 families [13] in 2 patients presenting with steroid-resistant nephrotic syndrome and FSGS. One patient harboring the Y47* mutation was diagnosed with MCD; however, he progressed to chronic kidney disease (CKD) stage 1 in 4 years, ruling out MCD and strongly suggesting FSGS. FSGS-associated variants D388H and K604*, as well as several mutations found in patients with steroid-resistant nephrotic syndrome but without a definitive FSGS diagnosis, were identified in a large-scale sequencing survey of patients with steroid-resistant nephrotic syndrome [14]. The leading presentation was nephrotic range proteinuria and nephrotic syndrome in 10/11 patients; 1/11 patients showed subnephrotic proteinuria, and in 1 patient, proteinuria was "++++" (Table 1). Hematuria, typically microhematuria, was detected in 3/6 patients where its presence was specifically noted. Kidney failure developed in 4/9 patients where the patient was followed clinically 1–13 years after the initial presentation; the average age at kidney failure was 13 years. The index biopsy resulting in the histological diagnosis of FSGS was always done at the point of initial presentation except for two patients, where the kidney biopsy was done 3 years after the onset of symptoms. Mesangial expansion or "hyperplasia" were noted in 4/6 patient biopsies where such data was available. Concomitant tubulointerstitial changes were reported in 4 patients and consisted of mild interstitial fibrosis and tubular atrophy. Electron microscopy description was available only in 1 published patient [5], highlighting podocyte and GBM alterations similar to those described in patients 1 and 2 and noting mesangial expansion.

Several patients had a ciclosporin-associated reduction in proteinuria [5]. Eight patients received treatment with steroids, ciclosporin, cyclophosphamide, and ACE inhibitors in various combinations (most common steroids, ciclosporin, and ACE inhibitors). Four of them demonstrated a reduction in proteinuria, but complete remission was not achieved.

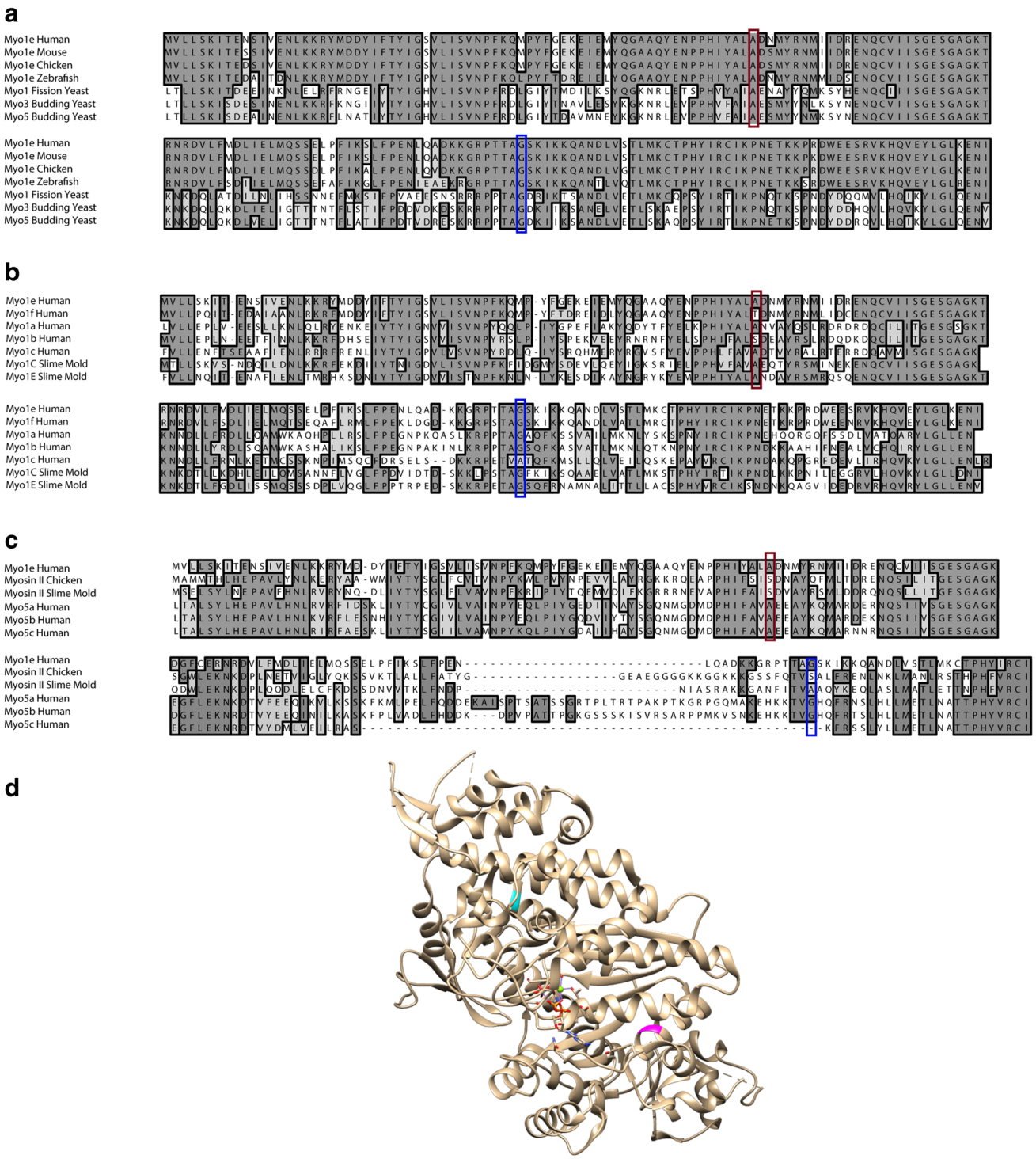

Discussion

The known homozygous FSGS-associated *MYO1E* missense mutations are located in the subdomains important for nucleotide binding and hydrolysis (P-loop, Switch 1, Switch 2). Deletion mutations prevent the expression either of most of the motor domain or its C-terminal part, including the actin-binding and converter regions along with the neck and tail domains. Our patient 2 is an example of the latter (Fig. 1). In addition, we have identified two missense variants in *MYO1E* that alter highly conserved amino acid residues in the myosin motor domain. Of the three variants described in this study, the two missense mutations can be classified as variants of uncertain significance (VUS)

◂**Fig. 3** Amino acid sequence alignments reveal the conservation of amino acid residues affected by disease-associated mutations within class I myosins (**a**, **b**). All known FSGS-associated *MYO1E* mutations involve the motor domain. **a** Human Myo1e (NP_004989.2) was aligned with Myo1e homologs from other species, including Myo1e from mouse, chicken, and zebrafish (AAH51391.1, XP_413782.4, NP_956930.1) and homologous class I myosins from fission yeast *S. pombe* (Myo1, NP_595402.1) and budding yeast *S. cerevisiae* (Myo3 and Myo5, P36006.4, Q04439.1). **b** Human Myo1e was aligned with its closest homolog in humans, Myo1f (NP_036467.2), short-tailed class I myosins, Myo1a, Myo1b, and Myo1c (NP_001242970.1, NP_036355.2, NP_203693.3), and long-tailed class I myosins, Myo1C and myo1E, from slime mold *Dictyostelium discoideum* (XP_643060.1, XP_636580.1). **c** Human *MYO1E* was aligned with myosin II heavy chains from chicken and *Dictyostelium discoideum* and with human myosins 5a, 5b, and 5c (P13538.4, XP_637740.1, NP_001369277.1, NP_001073936.1, XP_016877897.1). Red boxes in **a**, **b**, and **c** indicate amino acid residue A92 in Myo1e, while blue boxes indicate amino acid residue G562. A92 is conserved in all Myo1e homologs (**a**), as well as in the short-tailed myosins Myo1a and Myo1c (**b**), long-tailed class I myosins from *D. discoideum*, *S. pombe*, and *S. cerevisiae* (**b**), and in myosin 5 isoforms (**c**). G562 is conserved in all class I myosins examined except Myo1c, where it is replaced by a non-polar amino acid valine (**a** and **b**). Myosins II and 5a, 5b also contain a valine in the position corresponding to G562 (**c**). **d** Crystal structure of *D. discoideum* MyoIE (PDB 1LKX) was used to identify amino acid residues homologous to myo1e A92 (magenta) and G562 (cyan)

according to the ACMG guidelines [15], while one is predicted to be pathogenic (Table 2). The missense variants described here will require further functional studies for definitive classification. Overall, most FSGS-associated mutations affect the motor domain of Myo1e. The exact location and nature of the given *MYO1E* mutation do not affect the presentation or prognosis.

Of the clinicopathological manifestations of Myo1e-associated kidney disease, the most characteristic and striking are the diffuse global irregular GBM thickening, lamina densa multilayering, microgranular inclusions, and podocyte damage. This unique phenotype is seen when the ultrastructural data is available, such as in patient 1, patient 2, and one previous patient report [5], as well as in Myo1e-knockout experiments [2, 5]. A hallmark of Alport syndrome [16], these characteristic lesions are thought to accumulate due to the inability of the GBM lacking the Collagen IV α3, 4, and 5 isoforms to resist the changes in the intracapillary pressure and the resulting adaptive reaction of the podocytes, and endothelial and mesangial cells to the excessive biomechanical forces (reviewed in [17]). The slowly progressing structural disorganization of the GBM leads to gradual deterioration of the podocyte architecture and eventually FSGS.

Severe global "Alport-like" GBM disruption is seen in Myo1e-associated FSGS despite the absence of known biochemical GBM abnormalities. There is no early GBM thinning stage such as that seen in the Alport syndrome [16, 18], and only short areas of thinning GBM are seen; accordingly, hematuria may not be present. These patients may become proteinuric early in life, with the earliest pathological changes being, in addition to the GBM abnormalities, altered podocyte architecture and, already at this point, FSGS, focal global glomerulosclerosis, and interstitial "foam cells." Myo1e knockout mice develop the podocyte and GBM abnormalities already during the early postnatal phase of kidney development [2]. The average age at kidney failure in patients with Myo1e-associated FSGS is also significantly lower than that in Alport syndrome (23–25 years of age, with some variants as early as 10 years [19]). Thus, the dissimilarities in the initial presentation, time of FSGS onset, and time of progression to kidney failure between Alport syndrome and Myo1e-associated FSGS reflect the difference in histomorphology and can be used for the differential diagnosis. However, none of the clinical and histological features of the disease available so far is predictive of the clinical outcome.

Diffuse and global Alport-like changes are also detected in conditions affecting an important podocyte contractile actin cable component, non-muscle myosin 2a (Epstein and Fechtner syndrome) (e.g., [20, 21]), and upon interference with the actin cable attachment sites in an experimental knockout of the podocyte α3β1-CD151 adhesion complex in mice [22, 23]. A small GTPase, RhoA, maintains the podocyte contractile cable structure and attachment. Permanent activation of a RhoA-opposing GTPase Rac1 due to a mutation in a regulatory protein ARHGAP24 leads to segmental GBM lamination [24]. We analyzed the current genetic FSGS literature and did not find other conditions leading to diffuse and global Alport-like GBM changes, except for the renal-coloboma syndrome due to mutated podocyte *PAX2* [25] and Frasier syndrome caused by *WT1* mutation [26]. These mutations interfere with podocyte development, and their effect on the cytoskeleton is not known.

Myo1e is linked to regulation of cell-substrate adhesion [27–29] and may be necessary for podocyte attachment to the GBM [30]. Contractile actin cables in podocytes generate tension by pulling on the adhesion complexes and on the slit diaphragms, thus stabilizing the podocyte structure [31] and working in concert with the GBM to accommodate the hemodynamic capillary stress. We hypothesize that the GBM disorganization seen in Myo1e mutant kidneys represents an adaptational change in response to the inability of the podocyte cytoskeleton to maintain attachment to the GBM and tension. The synergism between the contractile actin system/adhesions/Myo1e and the GBM is demonstrated by the finding that when *MYO1E* mutations are encountered in the background of Alport syndrome, there is a much faster progression to kidney failure than that in respective individual conditions [32].

The first paper that described Myo1-associated FSGS suggested that ciclosporin can improve proteinuria in patients with Myo1e-associated FSGS, possibly due to its

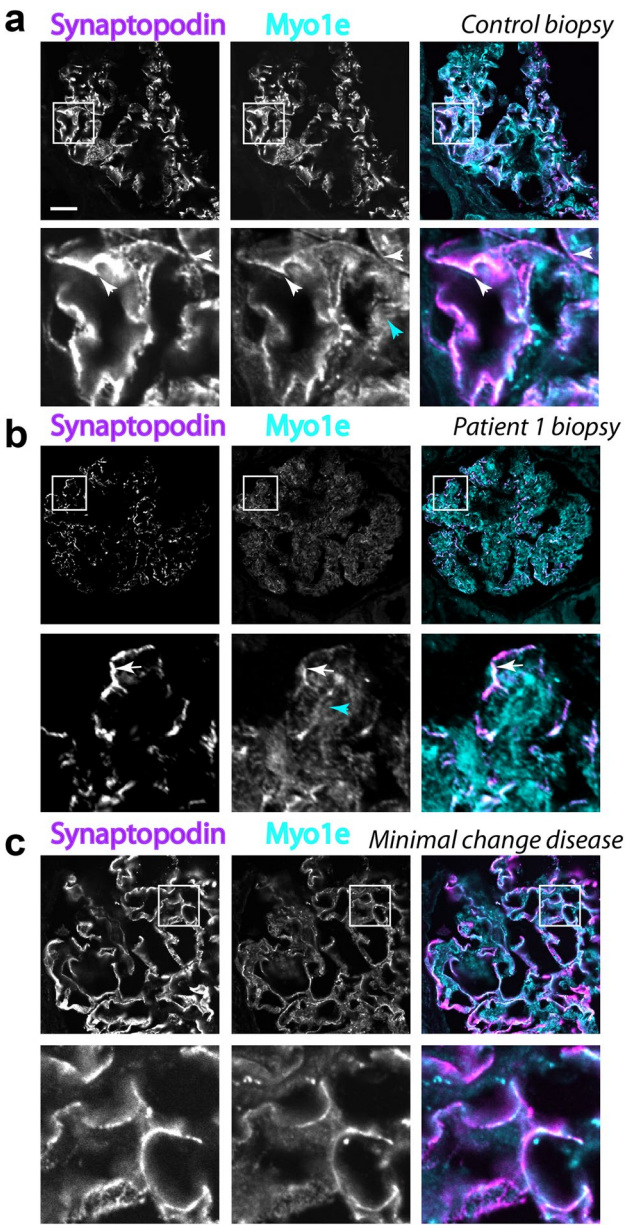

Fig. 4 Myo1e localization is disrupted in kidney biopsy samples from patient 1. (**a**, **b**, **c**) Single confocal sections of samples obtained from a control biopsy **a,** the diagnostic biopsy from the patient 1 **b**, and a patient with MCD **c**, stained with antibodies against synaptopodin and Myo1E. **a** In the control biopsy, both synaptopodin and Myo1E localize in a linear and punctate pattern along the glomerular basement membrane (white arrows), and Myo1E is also present in a more diffuse pattern in the cytoplasm of podocytes (blue arrow). **b** In the patient 1 biopsy, colocalization between synaptopodin and Myo1E (white arrow) is reduced, with the linear pattern of Myo1E staining being less pronounced than that in **a**. The majority of Myo1E is diffusely localized in the cytoplasm of podocytes (blue arrows). **c** In MCD, the localization and colocalization of synaptopodin and Myo1E are preserved. The right-hand panel shows combined synaptopodin (magenta) and Myo1e (cyan) staining with colocalizing pixels white. Lower panels in **a**, **b**, and **c** show enlargements of the boxed regions from the upper panels. Scale bar, 20 µm

stabilizing effect on the podocyte cytoskeleton [5]. Eleven years later, a wider selection of patients fails to confirm this (Table 1). However, it appears that therapy-associated reduction in proteinuria may be predictive of a better outcome.

Supplementary Information The online version contains supplementary material available at https://doi.org/10.1007/s00467-022-05634-x.

Acknowledgements We are grateful to Bjørn Westre, Department of Pathology, Ålesund Hospital, for contributing the first kidney biopsy of patient 2. We are indebted to the late Torunn Fiskerstrand from the Department of Medical Genetics, Haukeland University Hospital, Bergen. Without her, patient 2 would never have been correctly diagnosed. We thank Marie Claire Gubler, Laboratoire d'Anatomie Pathologique, Hopital Necker – Enfants Malades, Paris, for conducting the immunofluorescence investigation of a skin biopsy from patient 2 for collagen IV α chains. We thank Dmitry Lyalin, PhD, co-director of Cytogenetics/Molecular Genetics Laboratory, AHWFBMC, and Alicia Byrne, PhD, Clinical Genome Resource, Broad Institute of MIT and Harvard, for their advice and expert help with variant classification.

Funding This work was supported by the National Institute of Diabetes and Digestive and Kidney Diseases of the NIH under Award R01DK083345 to M.K. and by a pilot research award from the AHWF-BMC Department of Pathology to A.M.

Data availability No datasets were generated that would be necessary to interpret or replicate the findings in this article.

Declarations

Conflict of interest The authors declare no competing interests.

Ethics approval Approved by the Atrium Health Wake Forest Baptist Medical Center Institutional Review Board, ID IRB00063833.

Consent to participate Not required according to IRB; however, informed consent obtained from the patient's parents or the patient himself (patient 2).

Consent for publication Not required according to IRB. Consent for publication is given by patient 2.

References

1. McConnell RE, Tyska MJ (2010) Leveraging the membrane - cytoskeleton interface with myosin-1. Trends Cell Biol 20:418–426
2. Krendel M, Kim SV, Willinger T, Wang T, Kashgarian M, Flavell RA, Mooseker MS (2009) Disruption of Myosin 1e promotes podocyte injury. J Am Soc Nephrol 20:86–94
3. Bi J, Chase SE, Pellenz CD, Kurihara H, Fanning AS, Krendel M (2013) Myosin 1e is a component of the glomerular slit diaphragm complex that regulates actin reorganization during cell-cell contact formation in podocytes. Am J Physiol Renal Physiol 305:F532-544
4. Chase SE, Encina CV, Stolzenburg LR, Tatum AH, Holzman LB, Krendel M (2012) Podocyte-specific knockout of myosin 1e disrupts glomerular filtration. Am J Physiol Renal Physiol 303:F1099-1106

5. Mele C, Iatropoulos P, Donadelli R, Calabria A, Maranta R, Cassis P, Buelli S, Tomasoni S, Piras R, Krendel M, Bettoni S, Morigi M, Delledonne M, Pecoraro C, Abbate I, Capobianchi MR, Hildebrandt F, Otto E, Schaefer F, Macciardi F, Ozaltin F, Emre S, Ibsirlioglu T, Benigni A, Remuzzi G, Noris M, PodoNet Consortium (2011) MYO1E mutations and childhood familial focal segmental glomerulosclerosis. N Engl J Med 365:295–306
6. Skowron JF, Bement WM, Mooseker MS (1998) Human brush border myosin-I and myosin-Ic expression in human intestine and Caco-2BBe cells. Cell Motil Cytoskeleton 41:308–324
7. Schindelin J, Arganda-Carreras I, Frise E, Kaynig V, Longair M, Pietzsch T, Preibisch S, Rueden C, Saalfeld S, Schmid B, Tinevez JY, White DJ, Hartenstein V, Eliceiri K, Tomancak P, Cardona A (2012) Fiji: an open-source platform for biological-image analysis. Nat Methods 9:676–682
8. Ramage IJ, Howatson AG, McColl JH, Maxwell H, Murphy AV, Beattie TJ (2002) Glomerular basement membrane thickness in children: a stereologic assessment. Kidney Int 62:895–900
9. Kollmar M, Durrwang U, Kliche W, Manstein DJ, Kull FJ (2002) Crystal structure of the motor domain of a class-I myosin. EMBO J 21:2517–2525
10. Pettersen EF, Goddard TD, Huang CC, Couch GS, Greenblatt DM, Meng EC, Ferrin TE (2004) UCSF Chimera–a visualization system for exploratory research and analysis. J Comput Chem 25:1605–1612
11. van der Velde KJ, Dhekne HS, Swertz MA, Sirigu S, Ropars V, Vinke PC, Rengaw T, van den Akker PC, Rings EH, Houdusse A, van Ijzendoorn SC (2013) An overview and online registry of microvillus inclusion disease patients and their MYO5B mutations. Hum Mutat 34:1597–1605
12. Sanna-Cherchi S, Burgess KE, Nees SN, Caridi G, Weng PL, Dagnino M, Bodria M, Carrea A, Allegretta MA, Kim HR, Perry BJ, Gigante M, Clark LN, Kisselev S, Cusi D, Gesualdo L, Allegri L, Scolari F, D'Agati V, Shapiro LS, Pecoraro C, Palomero T, Ghiggeri GM, Gharavi AG (2011) Exome sequencing identified MYO1E and NEIL1 as candidate genes for human autosomal recessive steroid-resistant nephrotic syndrome. Kidney Int 80:389–396
13. Al-Hamed MH, Al-Sabban E, Al-Mojalli H, Al-Harbi N, Faqeih E, Al Shaya H, Alhasan K, Al-Hissi S, Rajab M, Edwards N, Al-Abbad A, Al-Hassoun I, Sayer JA, Meyer BF (2013) A molecular genetic analysis of childhood nephrotic syndrome in a cohort of Saudi Arabian families. J Hum Genet 58:480–489
14. Sadowski CE, Lovric S, Ashraf S, Pabst WL, Gee HY, Kohl S, Engelmann S, VegaWarner V, Fang H, Halbritter J, Somers MJ, Tan W, Shril S, Fessi I, Lifton RP, Bockenhauer D, El-Desoky S, Kari JA, Zenker M, Kemper MJ, Mueller D, Fathy HM, Soliman NA, Group SS, Hildebrandt F (2015) A single-gene cause in 295% of cases of steroid-resistant nephrotic syndrome. J Am Soc Nephrol 26:1279–1289
15. Richards S, Aziz N, Bale S, Bick D, Das S, Gastier-Foster J, Grody WW, Hegde M, Lyon E, Spector E, Voelkerding K, Rehm HL, Laboratory Quality Assurance Committee ACMG (2015) Standards and guidelines for the interpretation of sequence variants: a joint consensus recommendation of the American College of Medical Genetics and Genomics and the Association for Molecular Pathology. Genet Med 17:405–424
16. Gubler M, Levy M, Broyer M, Naizot C, Gonzales G, Perrin D, Habib R (1981) Alport's syndrome. A report of 58 cases and a review of the literature. Am J Med 70:493–505
17. Cosgrove D, Liu S (2017) Collagen IV diseases: a focus on the glomerular basement membrane in Alport syndrome. Matrix Biol 57–58:45–54
18. Cangiotti AM, Sessa A, Meroni M, Montironi R, Ragaiolo M, Mambelli V, Cinti S (1996) Evolution of glomerular basement membrane lesions in a male patient with Alport syndrome: ultrastructural and morphometric study. Nephrol Dial Transplant 11:1829–1834
19. Savige J, Storey H, Il Cheong H, Gyung Kang H, Park E, Hilbert P, Persikov A, Torres-Fernandez C, Ars E, Torra R, Hertz JM, Thomassen M, Shagam L, Wang D, Wang Y, Flinter F, Nagel M (2016) X-Linked and autosomal recessive Alport syndrome: pathogenic variant features and further genotype-phenotype correlations. PLoS One 11:e0161802
20. Moxey-Mims MM, Young G, Silverman A, Selby DM, White JG, Kher KK (1999) End-stage renal disease in two pediatric patients with Fechtner syndrome. Pediatr Nephrol 13:782–786
21. Kopp JB (2010) Glomerular pathology in autosomal dominant MYH9 spectrum disorders: what are the clues telling us about disease mechanism? Kidney Int 78:130–133
22. Kreidberg JA, Donovan MJ, Goldstein SL, Rennke H, Shepherd K, Jones RC, Jaenisch R (1996) Alpha 3 beta 1 integrin has a crucial role in kidney and lung organogenesis. Development 122:3537–3547
23. Baleato RM, Guthrie PL, Gubler MC, Ashman LK, Roselli S (2008) Deletion of CD151 results in a strain-dependent glomerular disease due to severe alterations of the glomerular basement membrane. Am J Pathol 173:927–937
24. Francis A, Burke J, Francis L, McTaggart S, Mallett A (2016) Polypoid change of the glomerular basement membrane in a child with steroid resistant nephrotic syndrome and ARHGAP24 mutation: a case report. Open Urol Nephrol J 9:88–93
25. Ohtsubo H, Morisada N, Kaito H, Nagatani K, Nakanishi K, Iijima K (2012) Alport-like glomerular basement membrane changes with renal-coloboma syndrome. Pediatr Nephrol 27:1189–1192
26. Ito S, Hataya H, Ikeda M, Takata A, Kikuchi H, Hata J, Morikawa Y, Kawamura S, Honda M (2003) Alport syndrome-like basement membrane changes in Frasier syndrome: an electron microscopy study. Am J Kidney Dis 41:1110–1115
27. Barger SR, Reilly NS, Shutova MS, Li Q, Maiuri P, Heddleston JM, Mooseker MS, Flavell RA, Svitkina T, Oakes PW, Krendel M, Gauthier NC (2019) Membrane-cytoskeletal crosstalk mediated by myosin-I regulates adhesion turnover during phagocytosis. Nat Commun 10:1249
28. Heim JB, Squirewell EJ, Neu A, Zocher G, Sominidi-Damodaran S, Wyles SP, Nikolova E, Behrendt N, Saunte DM, Lock-Andersen J, Gaonkar KS, Yan H, Sarkaria JN, Krendel M, van Deursen J, Sprangers R, Stehle T, Bottcher RT, Lee JH, Ordog T, Meves A (2017) Myosin-1E interacts with FAK proline-rich region 1 to induce fibronectin-type matrix. Proc Natl Acad Sci U S A 114:3933–3938
29. Gupta P, Gauthier NC, Cheng-Han Y, Zuanning Y, Pontes B, Ohmstede M, Martin R, Knolker HJ, Dobereiner HG, Krendel M, Sheetz M (2013) Myosin 1E localizes to actin polymerization sites in lamellipodia, affecting actin dynamics and adhesion formation. Biol Open 2:1288–1299
30. Mao J, Wang D, Mataleena P, He B, Niu D, Katayama K, Xu X, Ojala JR, Wang W, Shu Q, Du L, Liu A, Pikkarainen T, Patrakka J, Tryggvason K (2013) Myo1e impairment results in actin reorganization, podocyte dysfunction, and proteinuria in zebrafish and cultured podocytes. PLoS One 8:e72750
31. Suleiman HY, Roth R, Jain S, Heuser JE, Shaw AS, Miner JH (2017) Injury-induced actin cytoskeleton reorganization in podocytes revealed by super-resolution microscopy. JCI Insight 2:e94137
32. Lennon R, Stuart HM, Bierzynska A, Randles MJ, Kerr B, Hillman KA, Batra G, Campbell J, Storey H, Flinter FA, Koziell A, Welsh GI, Saleem MA, Webb NJ, Woolf AS (2015) Coinheritance of COL4A5 and MYO1E mutations accentuate the severity of kidney disease. Pediatr Nephrol 30:1459–1465